



## Research article

# Coeloglossum viride var. bracteatum extract attenuates staurosporine induced neurotoxicity by restoring the FGF2-PI3K/Akt signaling axis and Dnmt3

Zhe-Ping Cai<sup>a,1</sup>, Chang Cao<sup>a,1</sup>, Zhe Guo<sup>c,1</sup>, Yun Yu<sup>a</sup>, Si-Jia Zhong<sup>d</sup>, Rui-Yuan Pan<sup>a</sup>, Haowen Liang<sup>e</sup>, Rongfeng Lan<sup>b,\*</sup>, Xiao-Yan Qin<sup>a,\*\*</sup><sup>a</sup> Key Laboratory of Ecology and Environment in Minority Areas, National Ethnic Affairs Commission, Center on Translational Neuroscience, College of Life and Environmental Sciences, Minzu University of China, Beijing, 100081, China<sup>b</sup> Department of Cell Biology & Medical Genetics, School of Basic Medical Sciences, Shenzhen University Health Science Center, Shenzhen, 518060, China<sup>c</sup> The Emergency Department, The Third Affiliated Hospital of Guangxi Medical University, Nanning, 530021, China<sup>d</sup> College of Economics and Management, North China Electric Power University, Beijing, 102206, China<sup>e</sup> College of Letters & Science, University of California Los Angeles, CA, 90024, USA

## ARTICLE INFO

## Keywords:

CE  
Dnmt3a  
Dnmt3b  
FGF2  
PI3K/Akt  
Staurosporine

## ABSTRACT

We previously demonstrated the antioxidant activity of *Coeloglossum viride var. bracteatum* extract (CE) in rat cortical neurons and in mice with chemically induced cognitive impairment. In this work, we established a staurosporine (STS)-induced toxicity model to decipher the neuroprotective mechanisms of CE. We found that CE protected cell viability and neurite integrity in STS-induced toxicity by restoring the levels of FGF2 and its associated PI3K/Akt signaling axis. LY294002, a pan-inhibitor of PI3K, antagonized the activity of CE, although its-mediated restoration of FGF2 was unaffected. In addition, CE restored levels of Bcl-2/Caspase-3, PKC $\alpha$ /CaM pathway, and Dnmt3a and Dnmt3b, two methyltransferases that contribute to *de novo* DNA methylation. The Dnmts inhibitor 5-azacytidine impaired CE-mediated restoration of Dnmt3 or CaM, as well as the transition of DNA methylation status on the Dnmt3 promoter. These results reveal potential mechanisms that could facilitate the study and application of CE as a neuroprotective agent.

## 1. Introduction

The dried tuber of *Coeloglossum viride var. bracteatum* has long been used as food and medicine, and is documented as a superior tonic in classical Chinese medicine (Schubert et al., 2018). In recipes, it is used as a tonic to treat spermatorrhea and impotence, improve blood circulation, calm the mind, promote intelligence and prolong life (Shang et al., 2017). *Coeloglossum viride var. bracteatum* extract (CE) has been shown to enhance immunity, including antioxidant capacity, and enhance Alzheimer's disease (AD)-like mice in learning and memory (Guo et al., 2013; Ma et al., 2008; Pan et al., 2017; Qin et al., 2010; Zhang et al., 2006a). Pharmacological analysis has identified more than 120 compounds whose main components are glucosides, dihydrostilbenes, phenanthrenes, and aromatic compounds (Huang et al., 2004; Li et al., 2009; Shang et al., 2017). Among them, dactylorhin B exerts a protective effect against A $\beta$ <sub>25-35</sub>-induced toxicity in SH-SY5Y cells, which is a typical

toxin for AD development (Zhang et al., 2006c). We and colleagues have previously revealed the detoxification activity of CE in rat cortical and hippocampal neurons induced by A $\beta$ <sub>25-35</sub>, H<sub>2</sub>O<sub>2</sub>, NaNO<sub>2</sub>, ischemia and glutamate, etc (Guo et al., 2013; Ma et al., 2008; Pan et al., 2017; Qin et al., 2010). In particular, we recently found that CE has activity to improve learning and memory in mice with chemically induced cognitive impairment mice (Zhong et al., 2019). However, it is not clear how CE exerts these functions.

FGF2 (fibroblast growth factor 2) is a chemokine with broad mitogenic and cell survival-promoting activities in embryonic development, wound healing, cell migration and differentiation (Ford-Perriss et al., 2001; Johnson-Farley et al., 2007; Tomomi et al., 2011). The PI3K/Akt pathway is an intracellular signaling pathway that promotes metabolism, proliferation, and cell survival by mediating by serine and/or threonine phosphorylation of a number of downstream substrates in response to extracellular signals (Hemmings and Restuccia, 2012). Dysregulation of

\* Corresponding author.

\*\* Corresponding author.

E-mail addresses: [lan@szu.edu.cn](mailto:lan@szu.edu.cn) (R. Lan), [bjqinxiaoyan@muc.edu.cn](mailto:bjqinxiaoyan@muc.edu.cn) (X.-Y. Qin).<sup>1</sup> These authors contribute equally as the first authors.

the PI3K/Akt signaling pathway is seen in a variety of human diseases, including diabetes, cancer, cardiovascular disease, and neurological disorders (Hers et al., 2011). During neuroprotection, FGF2 binds to membrane receptors and activates the downstream PI3K/Akt or Erk1/2 signaling pathway, inducing expression of anti-apoptotic protein Bcl-2 but inhibiting activation of caspase-3 (Cheng et al., 2016; Pan et al., 2017). Thus, FGF2 attenuates A $\beta$ -induced toxicity in hippocampal neurons. In addition, FGF2 was recently reported to be an intracellular anti-apoptotic factor independent of FGFR activation and downstream signaling (Kostas et al., 2018). Therefore, FGF2 is a key regulator of neuronal survival and longevity.

Epigenetic modifications such as DNA methylation have been reported as a response to toxic brain injury (Zhao et al., 2013). DNA methylation frequently occurs in CpG islands of the genome, where methyl transfer to cytosine nucleotides is catalyzed by enzymes (Okano et al., 1999; Rhee et al., 2000). DNA (cytosine-5)-methyltransferase (Dnmt) is responsible for DNA methylation in mammals. However, Dnmts operate in different ways. Dnmt3a and Dnmt3b mainly mediate *de novo* methylation, while Dnmt1 prefers to methylate hemimethylated DNA. During STS-induced apoptosis in cancer cells, Dnmt3b is down regulated (Zhao et al., 2013). In contrast, Dnmt3a is essential for the long-lasting effects of cocaine in the nucleus accumbens of mouse, suggesting an important role in regulating cellular and behavioral plasticity in response to emotional stimuli (Cannella et al., 2018; LaPlant et al., 2010). Thus, epigenetic modifications and regulators play an indispensable function in neuropharmacology and drug development.

Staurosporine (STS) has a strong but non-selective inhibitory effect on protein kinase C (PKC) and other kinases, leading to cytotoxicity and induction of apoptosis (Qin et al., 2012; Zhao et al., 2013). Therefore, we used STS to establish an *in vitro* cellular model to investigate neuroprotective agents. We have previously demonstrated that STS-induced neurotoxicity can be attenuated by extract of *Polygonum multiflorum* (*He shou wu*, a traditional Chinese medicine known for its anti-aging properties) in cultured hippocampal neurons (Yang et al., 2014). In this study, STS was used to introduce toxicity and induce apoptosis in cultured hippocampal neurons to establish a cellular model to decipher the neuroprotective effects of CE. Special emphasis was placed on the CE-mediated regulation of *de novo* DNA methylation.

## 2. Materials and methods

### 2.1. Cultured hippocampal neurons

Rat primary hippocampal neurons were prepared as described previously (Cheng et al., 2016; Pan et al., 2017). The experimental methods were performed according to the guidelines approved by the Animal Care and Use Committee, Minzu University of China. Briefly, DIV1 (day *in vitro*), hippocampus of neonatal Sprague-Dawley (SD) rats was isolated under aseptic conditions, mechanically fragmented, and digested with 0.25% trypsin (Invitrogen) at 37 °C for 30 min. Digestion was terminated with DMEM containing 10% fetal bovine serum (FBS). The mixture was then filtered through a nylon mesh (mesh number = 70) and centrifuged at 1,500 rpm for 5 min to collect neurons. Neurons were suspended in DMEM containing 10% FBS, 2 g/L HEPES, penicillin G (100 U/mL) and 100  $\mu$ g/mL streptomycin (Invitrogen), seeded onto poly-L-lysine-coated plates or coverslips with a cell density of  $1 \times 10^6$  cells/mL, and incubated at 37 °C in a 5% CO<sub>2</sub> incubator. DMEM medium was used for the first 5 days, and then (DIV6) replaced with neural medium containing B-27 supplement in half the volume every two days. Neurons were used in the experiments in DIV7.

### 2.2. CE

Dried tubers (1.0 kg) of *Coeloglossum viride var. bracteatum* were extracted with 70% ethanol by reflux as described (Li et al., 2009; Ma et al., 2008; Zhang et al., 2006a, 2006b). The extracts were suspended in

water and partitioned successively with petroleum ether, ethyl acetate, and n-butanol. The n-butanol extract was then passed through HP-20 macroporous resin (#M0043, Solarbio) to obtain a 40% ethanol fraction. After removal of the solvent, the extract was weighed and suspended in water for use. The fractions were analyzed and confirmed using an YMC Hydroshere C18 column (4.6 mm  $\times$  250 mm, HS12S05-2546WT) equipped with an Agilent 1260. The four main components, Dactylorhin A, Dactylorhin B, Loriglossin, and Militarine, were characterized and confirmed (Supplementary Material Figures S1–3).

### 2.3. Chemicals

Staurosporine (#569397, non-selective kinase inhibitor of PKC, 0.2  $\mu$ M in use) and Dnmts inhibitor 5-azacytidine (5-AZ, #A2385, 0.4  $\mu$ M in working solution) were obtained from Sigma-Aldrich. The pan-PI3K inhibitors LY294002, (#9901, 10  $\mu$ M in use) and U0126 (#9903, 10  $\mu$ M in use) were provided by Cell Signaling Technology, Inc.

### 2.4. MTT cell viability assay

Prior to the experiment, neurons were isolated and cultured in 96-well plates for 6 days. After drug administration, the medium was replaced with medium containing 0.5 mg/mL of MTT (3-(4,5-dimethylthiazol-2-yl)-2,5-diphenyltetrazolium bromide) and further cultured for 3–4 h. Finally, the medium was removed and 100  $\mu$ L DMSO was added to completely dissolve the resulting formazan. The absorbance was recorded at 492 nm using a microplate spectrophotometer (Bio-Rad).

### 2.5. LDH determination

The lactate dehydrogenase (LDH) assay was performed using the CytoTox96 Non-Radioactive Cytotoxicity Assay kit (Promega). LDH is a cellular enzyme released in response to apoptosis or membrane damage. The released LDH was measured enzymatically by conversion of tetrazolium to formazan according to the manufacturer's instructions. The absorbance of the formazan solution was determined similarly in MTT.

### 2.6. TUNEL assay

Terminal deoxynucleotidyl transferase-mediated dUTP nick-end labeling (TUNEL) was used to quantify apoptotic cells by measuring the 3'-OH of DNA strand breaks. Cells were fixed with 4% paraformaldehyde for 15 min at room temperature and permeabilized with 0.2% Triton X-100 for 25 min. Cells were then subjected to TUNEL assay using the *in situ* cell death assay kit I (Roche) according to the manufacturer's instructions. The ratio of TUNEL-positive cells/DAPI-positive cells represents the rate of cell death. Images were obtained by a Leica SP8 confocal microscope, and three images were obtained for each group.

### 2.7. Western blot

Neurons were collected and protein were extracted with RIPA lysis buffer (#P0013C, Beyotime Biotechnology) containing 1% phenylmethylsulfonyl fluoride (PMSF, Roche) and then centrifuged at 4 °C, 13,000 rpm for 25 min. Proteins were collected and separated by 10% SDS-PAGE and then transferred to PVDF membranes. The primary and secondary antibodies were subsequently incubated. Primary antibodies were as follows: anti Akt (#9272), phospho-Akt (Ser473) (#4060), Bcl-2 (#3498),  $\beta$ -actin (#4970) and cleaved-Caspase-3 (#9662) antibodies were purchased from Cell Signaling Technology, Inc. Anti-Dnmt1 (#ab188453), Dnmt3b (#ab79822), CaM (#ab2860), phospho-Erk1/2 (#ab200807), and Erk1/2 (#ab184699) antibodies were purchased from Abcam plc. Anti-Dnmt3a (#20954-1-AP) antibody was purchased from Proteintech Group, Inc. Anti PKC $\alpha$  (#sc-17769) antibody was supplied by Santa Cruz Biotechnology and FGF2 (#SAB2100814) was

purchased from Sigma-Aldrich. Western blot images were obtained from the Odyssey CLx infrared fluorescence imaging system (LI-COR Biosciences). The relative optical density of the blotted bands was quantified using Image J software, and relative protein levels were calculated.

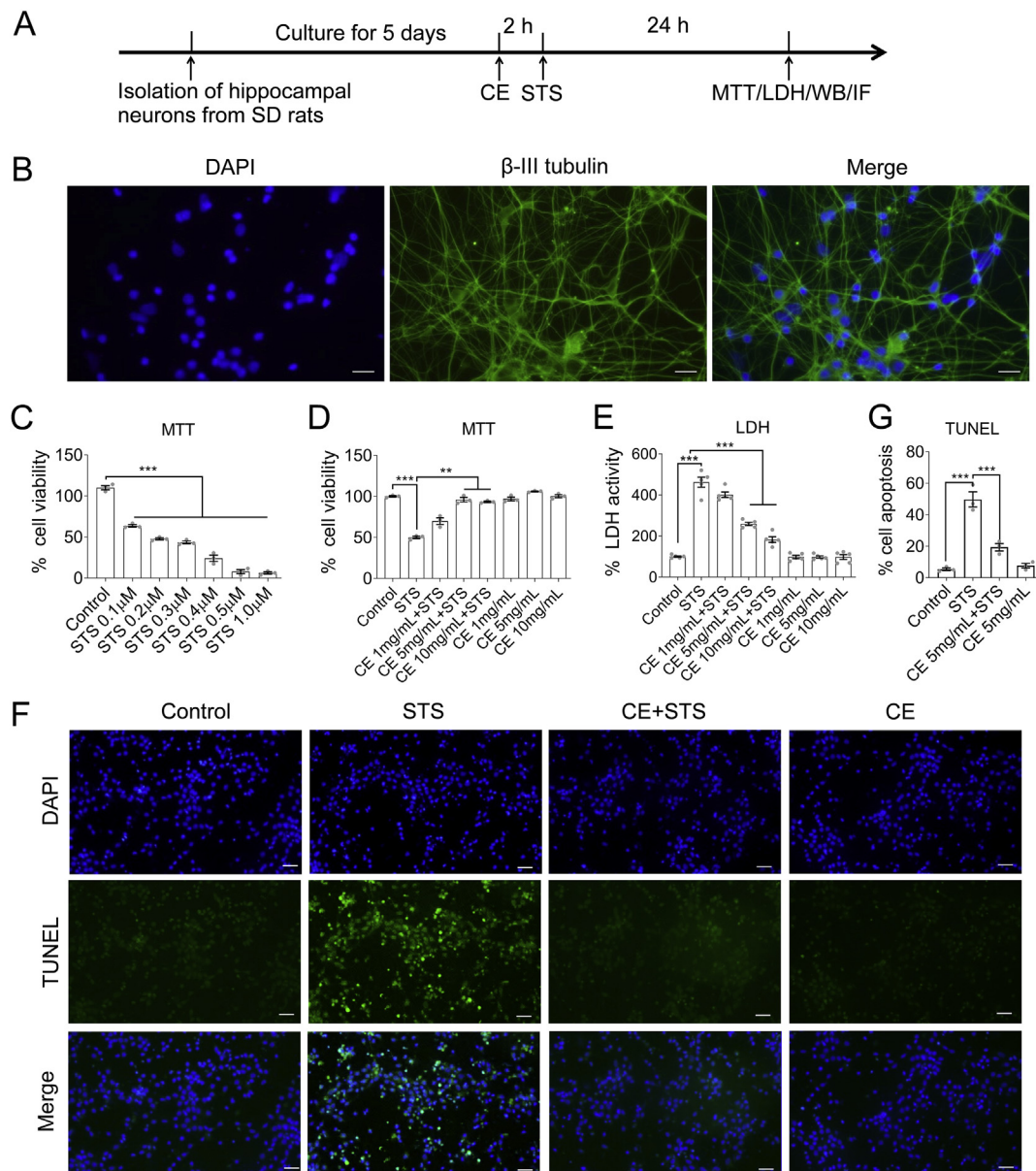
## 2.8. Immunofluorescence

After experimental treatment, neurons seeded on 24-well plates with coverslips were subjected to immunofluorescence. Cells were fixed with 4% paraformaldehyde for 15 min and then incubated for 1 h in blocking buffer (PBS containing 5% serum and 0.3% Triton X-100), followed by incubation with the primary antibody  $\beta$ -III tubulin (dilution 1:500, #T8578, Sigma-Aldrich) or MAP2 (1:1000, #T8578, Sigma-Aldrich) overnight at 4 °C. After washing 3 times with PBS, neurons were

incubated with Alexa Fluor 488 or 546-conjugated secondary antibodies (Invitrogen) for 1.5 h at room temperature, rinsed 3 times with PBS and stained with DAPI (4',6-diamidino-2-phenylindole) for 15 min. Images were obtained using a Leica SP8 confocal microscope. The length of neurite was measured by Image J.

## 2.9. Methylation-specific PCR

Methylation-specific PCR was performed on CpG islands within gene targets using the bisulfite conversion method (TIANGEN Biotech (Beijing) Co., Ltd.) as described previously (Herman et al., 1996). Briefly, 500 ng of genomic DNA purified with the TIANamp Genomic DNA Kit (#DP304) was converted by the DNA bisulfite conversion kit (#DP215) for transformation. To amplify the methylated sequences, PCR was



performed on 20 ng of bisulfite-transformed DNA using MSP DNA polymerase from the Methylation-specific PCR Kit (EM101) with specific primers (Supplementary Table S3). The PCR product (10  $\mu$ L) was loaded onto a 1% agarose gel, stained with GelRed (Biotium), and visualized under UV illumination.

### 2.10. Statistical analysis

Results are expressed as mean  $\pm$  s.e.m. Statistical differences between groups were determined by one-way analysis of variance (ANOVA) and Tukey's multiple comparison tests in GraphPad Prism 7.0 software. n.s, not significant; \*,  $p < 0.05$ ; \*\*,  $p < 0.01$ ; \*\*\*,  $p < 0.001$ .

## 3. Results

### 3.1. CE attenuates STS-induced toxicity and apoptosis in hippocampal neurons

To determine the neuroprotective effects of CE, we established a model of STS-induced cytotoxicity and apoptosis in hippocampal neurons. Hippocampal neurons were newly isolated from neonatal Sprague-Dawley rats (Figure 1A). The purity of hippocampal neurons was examined by immunofluorescence using an antibody against the neuron-specific marker  $\beta$ -III tubulin (Figure 1B, Supplementary Material Figure S5). The purity of hippocampal neurons exceeded 90% and was considered to meet the experimental requirements. In establishing the STS-induced cytotoxicity model, hippocampal neurons were incubated with set concentrations of STS (0.1–1  $\mu$ M) and their cell viability was measured (Figure 1C). Accordingly, we concluded that 0.2  $\mu$ M of STS is a reasonable concentration to induce cytotoxicity and apoptosis in hippocampal neurons, where cell viability is reduced to 50%. Also, the optimal concentration of CE for neuroprotection was determined. 5 or 10 mg/mL of CE had a significant protective effect on hippocampal neurons with no measurable adverse effect on cell viability (Figure 1D). In the next study, we used 5 or 10 mg/mL of CE and 0.2  $\mu$ M of STS to explore the neuroprotective mechanism of CE. In addition, we performed LDH assay and TUNEL assay, respectively. CE attenuated STS-mediated toxicity at concentrations of 5 or 10 mg/mL (Figure 1E). The TUNEL assay showed that CE significantly abrogated STS-induced apoptosis, narrowing cell mortality from 50% to 20% (Figure 1F and G). Thus, we established a model of STS-mediated hippocampal neurotoxicity and confirmed the neuroprotective effect of CE.

### 3.2. CE protects neuronal integrity, neurite outgrowth and extension from STS-induced toxicity

To verify the protective effect of CE against STS-induced toxicity, neurons were immuno-labeled with antibodies against microtubule-associated protein 2 (MAP2), a protein that regulates neuronal

morphogenesis and organelle transport in neurites (Dehmelt and Halpain, 2005). STS clearly compromised cell body integrity and led to neurite fragmentation (Figure 2A, Supplementary Material Figure S6), indicating that although the cells did not die, neuronal function was significantly affected. In contrast, CE rescued neurons from STS-induced morphological collapse and preserved their neurite outgrowth and extension (Figure 2, CE + STS column). Thus, CE maintains the integrity of the cell body and the continuity of neurite.

### 3.3. The FGF2-PI3K/Akt signaling axis is required for the neuroprotective activity of CE

It has been previously reported that CE has antioxidant or anti-amyloid neurotoxic activity by restoring the PI3K/Akt signaling axis (Pan et al., 2017; Qin et al., 2010). Therefore, we used the pan-PI3K inhibitor LY294002 (working concentration of 10  $\mu$ M) to elucidate the mechanism of CE mediated neuroprotective function (Figure 3A). In STS-treated neurons, FGF2, phosphorylation of Akt and Erk1/2 was significantly down-regulated, while the apoptotic indicator cleaved-Caspase-3 (cleaved-Casp-3) was apparently elevated, while the anti-apoptotic protein Bcl-2 was decreased (Figure 3B–F, Supplementary Material Figure S7). However, CE effectively rescued FGF2 expression and reactivated Akt or Erk1/2 (p-Akt, p-Erk1/2) as well as Bcl-2 (Figure 3B–E). In contrast, cleaved-Casp-3 was clearly abolished. Thus, CE ameliorated the expression of FGF2, Akt, and Bcl-2/cleaved-Casp-3 to antagonize STS-induced toxicity. However, by pretreating neurons with LY294002 prior to CE and STS treatment to inhibit PI3K and its downstream Akt signaling pathway, we unexpectedly observed that CE-mediated rescue of cell viability was inhibited (Figure 3G, STS + CE + LY column). Consistently, the activation of Akt (p-Akt) was apparently also eliminated (Figure 3H). However, CE was able to rescue FGF2 expression despite the inhibition of the Akt signaling pathway (Figure 3I), because FGF2 is located upstream of the PI3K/Akt pathway. In other words, CE regulates FGF2 expression independently of PI3K/Akt signaling. Furthermore, Erk1/2 activity was rescued by CE and blocked by Erk1/2 inhibitor U0126 (Figure 3J). However, U0126 did not impair CE-mediated restoration of cell viability (Figure 3G), and therefore Erk1/2 activity was not essential in CE-mediated neuroprotection. Therefore, we suggest that the FGF2-PI3K/Akt signaling axis plays an essential role in the neuroprotective effects of CE in response to STS-induced toxicity.

### 3.4. Dnmt3a and Dnmt3b are involved in CE-mediated neuroprotective functions

There is compelling evidence that neurotoxicity of harmful substances can modulate epigenetic modifications, including methylation, acetylation or ubiquitination (Hu and Su, 2017). Neurotoxins are thought to cause DNA hypomethylation and in this way enable the expression of downstream genes. With this in mind, we intended to test whether DNA

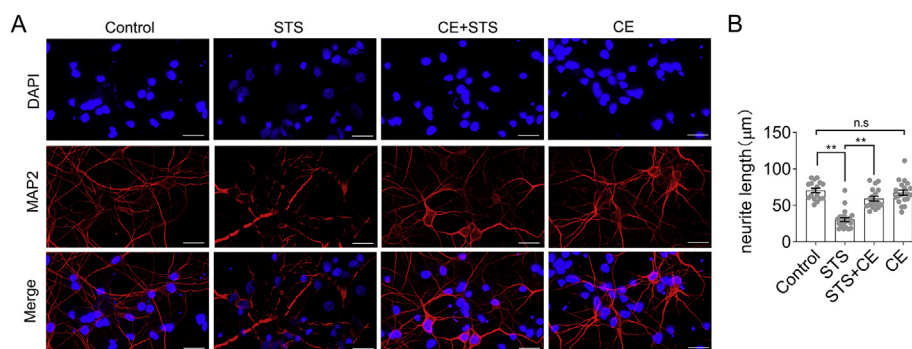


**Figure 2.** CE protects neuronal cell body integrity, neurite outgrowth and extension from STS-induced toxicity. (A) Neurons were incubated with STS (0.2  $\mu$ M) and CE (5 mg/mL) and immuno-labeled with MAP2 antibody. STS compromised cell body integrity and caused neurite shortening, indicating impaired neuronal activity. In contrast, CE rescued neurons from STS-induced toxicity, while CE alone did not introduce observable toxicity. Scale bar = 25  $\mu$ m. Nuclei were stained with DAPI. (B) The length of neurite was calculated by Image J ( $n > 17$ ). Data are shown as mean  $\pm$  s.e.m. Statistical significance of difference between groups was examined by one-way ANOVA followed by Tukey's multiple comparison tests. \*\*,  $p < 0.01$ ; n.s, not significant. Non-adjusted images were presented in Supplementary Material Figure S6.

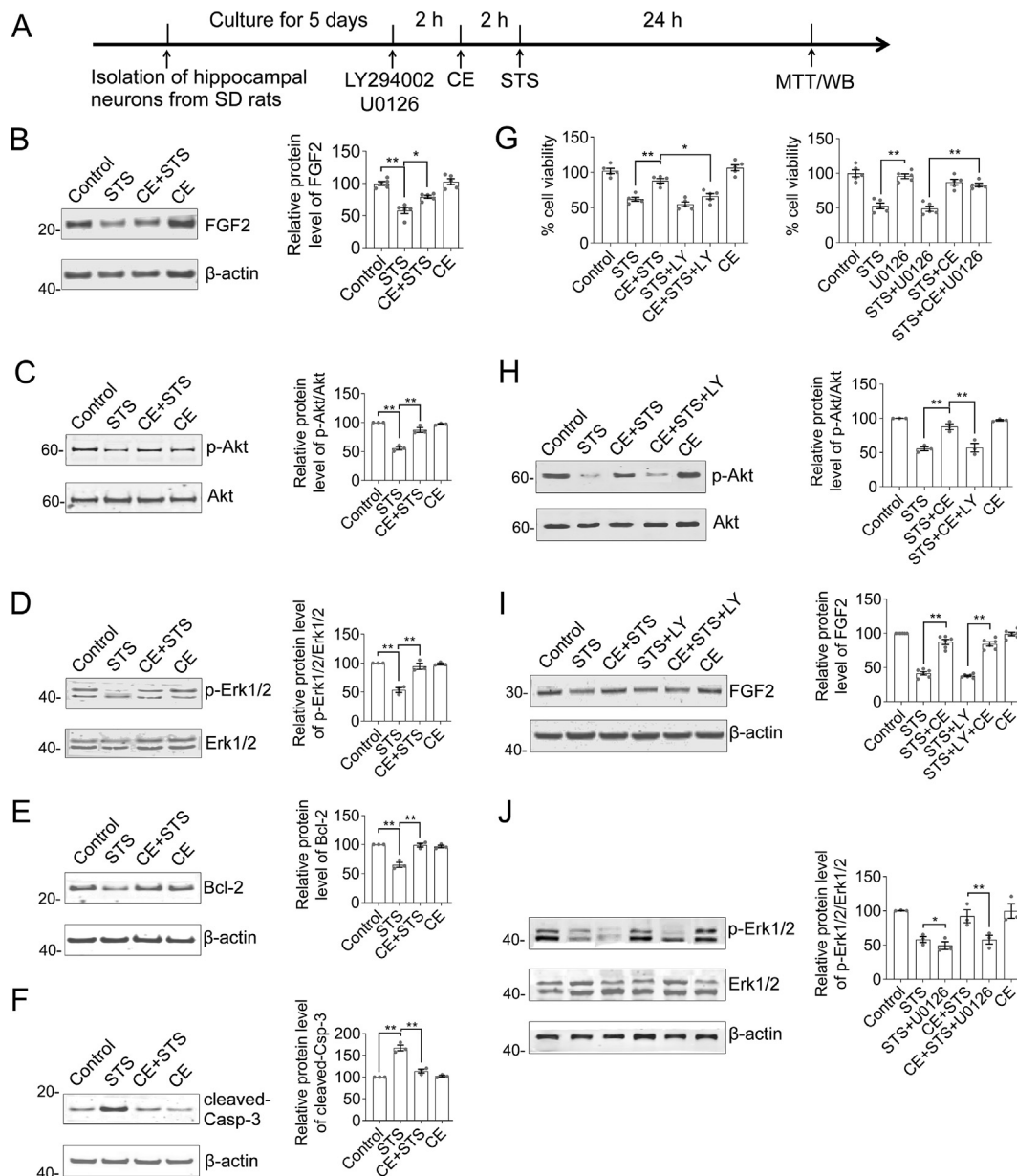


**Figure 3.** CE restores the FGF2-Akt, Erk1/2 signaling axis and Bcl-2/caspase-3 apoptotic pathway to protect neurons from STS-induced toxicity. (A) Experimental timeline. Hippocampal neurons were incubated with LY294002 (PI3K inhibitor) or U0126 (Erk1/2 inhibitor), STS or CE as indicated, followed by Western blot and MTT cell viability assay. (B–F) Representative blots of FGF2, Akt, Erk1/2, Bcl-2, and cleaved-Casp-3. STS induced a decrease in FGF2 levels, inhibited the FGF2-Akt/Erk1/2 pathway and turned on the apoptotic pathway. In contrast, CE restored FGF2 expression, reactivated the Akt/Erk1/2 pathway, and eliminated activation of the apoptotic pathway. Relative protein levels of FGF2, Bcl-2 and cleaved-Casp-3 were normalized to  $\beta$ -actin, whereas p-Akt and p-Erk1/2 were normalized to their total protein (Akt or Erk1/2), respectively. (G) MTT cell viability assay of neurons incubated with STS, CE, LY294002, or U0126 as indicated. LY294002 but not U0126 antagonized the neuroprotective effect of CE on STS-induced toxicity. (H–J) Representative blots of Akt, FGF2, and Erk1/2. Inhibition of the PI3K/Akt pathway (via LY294002) abrogated CE-mediated rescue of p-Akt, but did not affect CE-mediated recovery of FGF2. In this figure, results are expressed as mean  $\pm$  s.e.m. One-way ANOVA and Tukey's multiple comparison tests were performed to examine statistical significant differences between groups ( $n = 5$ ). \*,  $p < 0.05$ ; \*\*,  $p < 0.01$ . Non-adjusted blots were presented in Supplementary Material Figure S7.

methyltransferases are involved in CE-mediated neuroprotective functions. 5-azacytidine (5-AZ), an analog of cytidine, effectively inhibits DNA methyltransferase and induces DNA hypomethylation (Jiemjit et al., 2008; Yang et al., 2017). In the experiments, neurons were pretreated with 5-AZ followed by STS or CE treatment (Figure 4A and B, Supplementary Material Figure S8). As observed from microscopic imaging and MTT cell viability assay, the cell viability of the CE + STS+5-AZ group was significantly better than that of STS or STS+5-AZ group and comparable to that of the CE + STS group (Figure 4C). In other words, 5-AZ did not synergize with STS to inhibit cell viability. However, we observed

that STS down-regulated the expression of Dnmt1, Dnmt3a and Dnmt3b, while in contrast, the addition of CE rescued the expression of Dnmt3a, Dnmt3b but not Dnmt1 (Figure 4D and E, Supplementary Material Figure S9). These results suggest that Dnmt3a and Dnmt3b may be downstream effectors that promote CE-mediated neuroprotective functions. Consistently, addition of 5-AZ prevented CE-mediated rescue functions of Dnmt3a and Dnmt3b (Figure 4E). The activity of Dnmt3a and Dnmt3b mainly contributes to *de novo* methylation of DNA (Okano et al., 1999). Thus, *de novo* methylation of DNA is thought to be involved in CE-mediated protection of neurons from STS-induced toxicity.

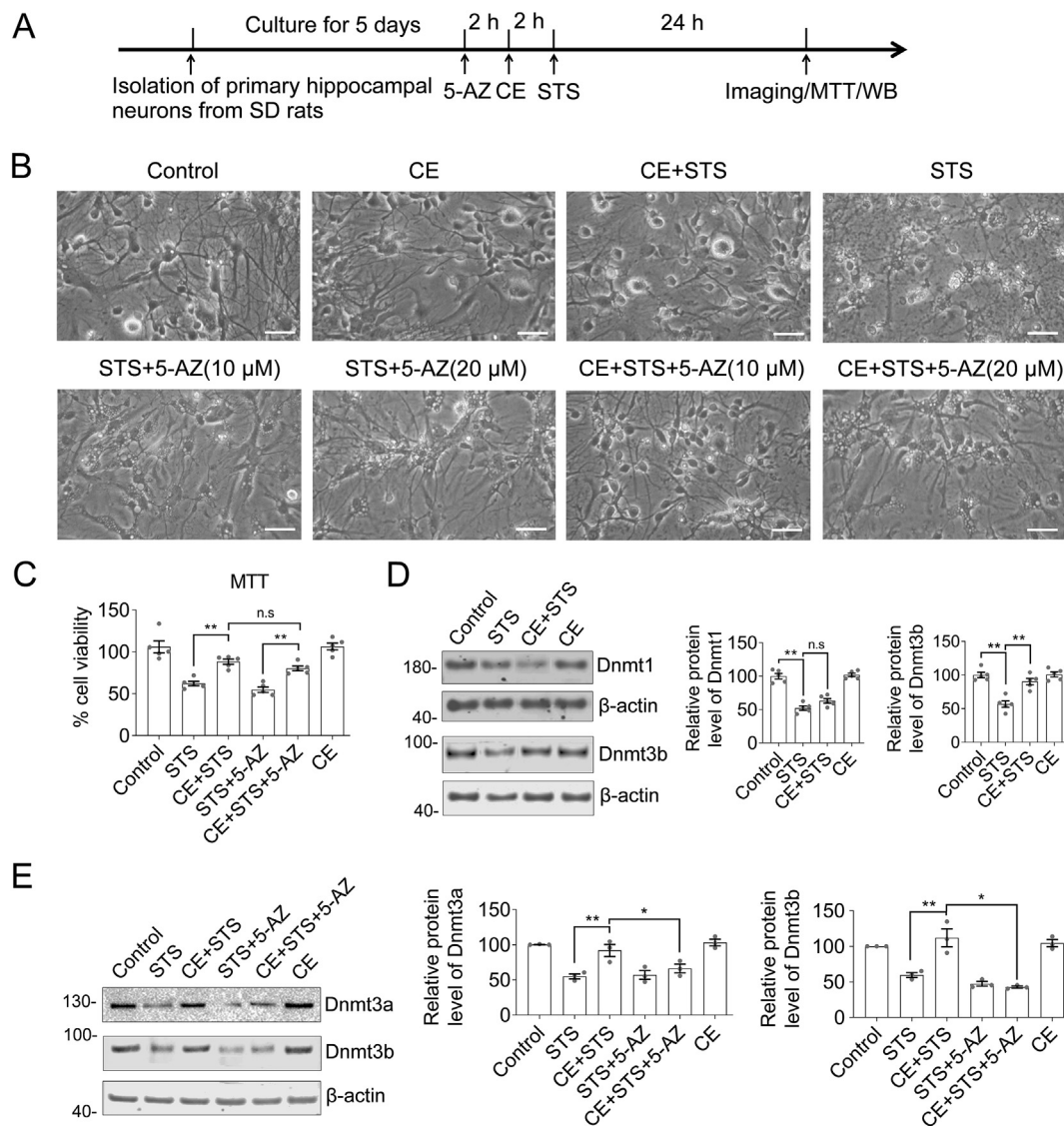


**Figure 4.** Dnmt3 is involved in CE-mediated neuroprotective effects. (A) Experimental timeline. Hippocampal neurons were incubated with 5-AZ (Dnmts inhibitor), STS or CE, followed by microscopic imaging, Western blot and MTT assay. (B) Images of drug-exposed neurons. Scale bar, 25  $\mu$ m. (C) MTT assay showing that inhibition of Dnmts did not inhibit CE-mediated protection against STS-induced toxicity.  $n = 5$ . (D) Representative blots of Dnmt3b and Dnmt1. Dnmt3b but not Dnmt1 was restored by CE to recover from STS-induced toxicity (CE + STS column). (E) Representative blots of Dnmt3a and Dnmt3b. Inhibition of Dnmts (by 5-AZ) prevented CE-mediated recovery of Dnmt3a and Dnmt3b. In D ( $n = 5$ ) and E ( $n = 3$ ), relative protein levels were calculated from the optical density of blots and normalized to  $\beta$ -actin. (C–E) Data are shown as mean  $\pm$  s.e.m. One-way ANOVA, post hoc Tukey's tests were performed. \*,  $p < 0.05$ ; \*\*,  $p < 0.01$ . n.s., not significant. Non-adjusted images and blots were presented in Supplementary Material Figures S8 and S9.

### 3.5. CaM may be a downstream effector of the protective process mediated by CE through restoration of DNA methylation

STS is a broad-spectrum protein kinase inhibitor that induces apoptosis mainly through inhibition of protein kinase C (PKC) activity (Omura et al., 1977). Therefore, we designed to investigate the function of the PKC/CaM signaling axis in CE-mediated neuroprotective function (Figure 5, Supplementary Material Figure S10). Calmodulin regulates a large number of enzymes, especially protein kinases and phosphatases, ion channels, aquaporins and other proteins through calcium binding. Western blotting showed that both PKC $\alpha$  and CaM (Calmodulin-2, also known as CALM2) were significantly down-regulated in STS-treated neurons (Figure 5A and B). However, the addition of CE effectively rescued the expression of PKC $\alpha$  and CaM (Figure 5A and B, CE + STS columns). These results suggest that CE restores the PKC $\alpha$ /CaM signaling axis in response to STS-induced toxicity. However, the way CE

rescues PKC $\alpha$  and CaM expression may behave differently. Dnmt3a and 3b, but not Dnmt1, are involved in the process of CE-mediated neuroprotective function (Figure 4). Neurons were incubated with 5-AZ to inhibit DNA methyltransferases (Dnmts) that cause DNA hypomethylation and promote transcription. Consistently, PKC $\alpha$  expression was rescued by the addition of 5-AZ or CE (Figure 5C, CE or 5-AZ column vs STS). However, STS-induced CaM down-regulation could not be rescued by CE (Figure 5D, CE + STS+5-AZ column). In other words, 5-AZ was able to replace the rescue of CaM by CE (Figure 5D). Moreover, CE rescued Bcl-2 expression to inhibit apoptosis with or without the addition of 5-AZ (Figure 5E). Thus, CaM may be a downstream effector involved in CE-mediated neuroprotective processes. Furthermore, methylation-specific PCR consistently showed that the regulation of gene expression by CE is mediated by methylation, especially for Dnmt3b (Figure 5F, Supplementary Material Figure S11). CE represses methylation of the Dnmt3b gene to promote its expression and

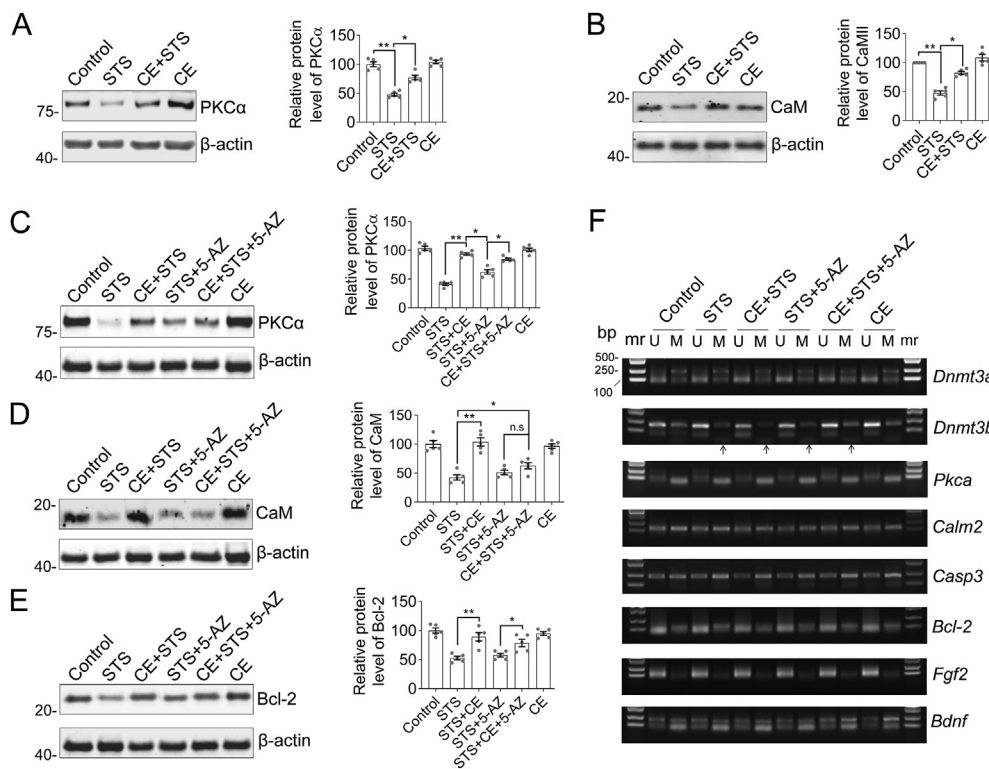


**Figure 5.** CE ameliorates the PKC $\alpha$ /CaM pathway to protect neurons from STS-induced toxicity. (A–B) Representative blots of PKC $\alpha$  and CaM. CE rescues STS-induced down-expression of PKC $\alpha$  and CaM. (C–E) Inhibition of Dnmts by 5-AZ impairs CE-mediated recovery of CaM but not PKC $\alpha$  and Bcl-2 expression. In A–E, results are shown as mean  $\pm$  s.e.m. Statistical significance of differences between groups was calculated by one-way ANOVA followed by Tukey's tests, n = 5. \*, p < 0.05; \*\*, p < 0.01; n.s, not significant. (F) Methylation-specific PCR suggests that promoter methylation of Dnmt3b is involved in CE-mediated neuroprotection. mr, DNA marker; U, unmethylated; M, methylated. Non-adjusted blots and gels were presented in Supplementary Material Figures S10 and S11.

can be inhibited by 5-AZ (Figure 5F, CE + STS vs STS). Thus, Dnmt3b activity may also be involved in CE-mediated neuroprotective functions.

In summary, FGF2 and its downstream PI3K/Akt and PKC $\alpha$ /CaM pathways and DNA methyltransferase Dnmt3b are involved in CE-mediated neuroprotective functions, synergistically maintaining Bcl-

2expression and inhibiting the apoptotic enzyme cleaved-Casp-3 (Figure 6).

#### 4. Discussion

The dried tuber of *Coeloglossum viride var. bracteatum* is an ancient Tibetan medicine that has long been used a medicine and food. In ethnomedicine, it is used as a reinforcing agent to invigorate the body and strengthen the Yang. Increasing attention and studies have demonstrated the antioxidant activity, immunomodulation, learning and memory enhancement, and antiviral activity of this ancient medicine (Shang et al., 2017). Several *Coeloglossum viride var. bracteatum* extracts were used in mouse models of dementia and Alzheimer's disease to verify antioxidant, metabolic modulating and anti-apoptotic effects (Ma et al., 2008; Zhang et al., 2006b). However, the pharmacological effects and characteristic chemicals and biological indicators of CE still need to be further developed.

We previously reported that CE has antioxidant, anti-glutamate and A $\beta$  effects on cultured cortical neurons (Pan et al., 2017; Qin et al., 2010). CE ameliorates learning and memory deficits in chemically induced mice by restoring neurotrophin expression and inhibiting pro-inflammation (Zhong et al., 2019). In this study, we established an STS-induced toxicity and apoptotic cell model based on hippocampal neurons to explore the signaling axis and potential epigenetic modifications of CE-mediated neuroprotective functions. Consistently, neurons cultured with STS exhibited collapse of neuronal bodies and neurites decay (Figures 1 and 2). Fortunately, CE rescued neurons from STS-induced morphological disorder and maintained cellular integrity and neurite continuity. In addition, there was no toxicity in neurons treated with 5–10 mg/mL CE relative to those administered with 0.2  $\mu$ M STS. Thus, we confirmed the neuroprotective effect of CE in promoting neuronal survival and plasticity. During the protection of neuronal survival and growth, the expression of cytokines such as FGF2 and BDNF was activated. Also, since FGF2 and BDNF usually act as signaling primers, the PI3K/Akt signaling axis is frequently activated from its background level in response to cellular stress. Indeed, we previously observed the

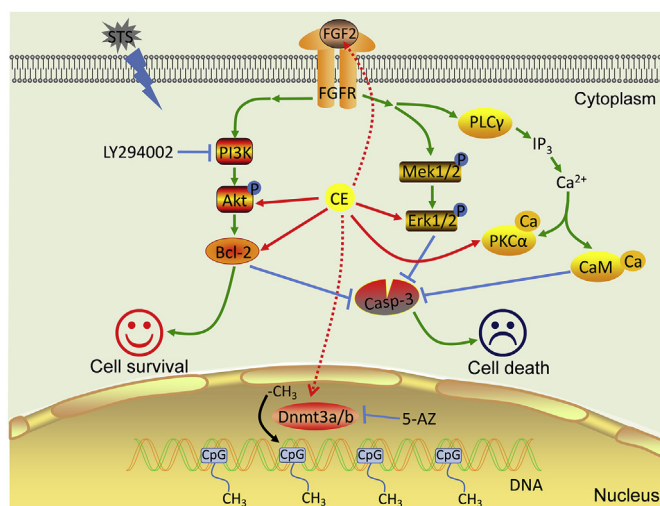


**Figure 6.** Schematic representation of CE-mediated neuroprotection against STS-induced toxicity. STS inhibits protein kinases and induces apoptosis and severe cytotoxicity to neurons. CE restores expression of FGF2, maintains the activity of PI3K/Akt, Erk1/2 and PKC $\alpha$ /CaM pathway, and promotes cell survival. The PI3K/Akt signaling pathway plays a role in CE-mediated function, as inhibition of PI3K/Akt by LY294002 is known to abrogate CE activity. Meanwhile, the cleaved-Casp-3 associated apoptotic pathway activated by STS was significantly attenuated by CE. In addition, DNA *de novo* methyltransferase activity may be involved in CE-mediated regulation of gene expression and can be inhibited by the Dnmts inhibitor 5-AZ, suggesting that epigenetic regulation is involved in CE-mediated neuroprotection processes.

activation of Akt signaling in CE-treated cells in response to H<sub>2</sub>O<sub>2</sub> or A $\beta$ -induced oxidative stress (Pan et al., 2017; Qin et al., 2010). However, CE is non-toxic and CE-treated healthy cells did not show significant signaling of the PI3K/Akt pathway. Therefore, in STS-treated neurons, we consistently observed restored expression of FGF2 after CE administration (Figure 3). FGF2 is a potent factor in activating PI3K/Akt, Erk1/2, and PKC $\alpha$ /CaM signaling pathways to promote cell survival (Ford-Perriss et al., 2001; Tomomi et al., 2011; Zhang and Yuan, 1998). Accordingly, inhibition of the apoptotic pathway, for antagonistic expression of Bcl-2 and cleaved-caspase-3 was restored. Inhibition of PI3K by LY294002 abrogated both activation of the downstream Akt signaling axis and the neuroprotective function of CE. However, CE-mediated expression of FGF2 was still retained (Figure 3). Furthermore, the sustained expression of FGF2 after CE incubation suggests an independent mechanism to induce FGF2 transcription in addition to neuroprotective pathways such as the PI3K/Akt signaling axis. Thus, the PI3K/Akt axis is one of the important signaling axes in CE-mediated neuroprotective function.

DNA methylation occurs at CpG dinucleotides and represses gene expression. Three DNA methyltransferases, Dnmt1, Dnmt3a and Dnmt3b, are responsible for this reaction. Recently, epigenetic modifications on DNA or histones have gained consideration in neuroscience regarding the mechanisms of substance abuse, depression and neurodegenerative diseases. Indeed, the importance of DNA methyltransferases such as Dnmt3a in the regulation of emotional behavior and spinal plasticity has been demonstrated (LaPlant et al., 2010). Dnmt3b is down-regulated in STS-induced apoptosis in hepatocarcinoma cells (Zhao et al., 2013). In general, Dnmt1 prefers to methylate hemimethylated DNA and maintain methylation, while Dnmt3a and Dnmt3b play a role in *de novo* methylation. In this study, we found that Dnmt3 (Dnmt3a and Dnmt3b), but not Dnmt1 exhibited responsive expression after CE incubation to eliminate STS-induced toxicity (Figure 4). Recently, Dnmt3a was reported to improve muscle atrophy in diabetic mice by activating Akt, suggesting that Dnmt3a could provide feedback to the PI3K/Akt signaling pathway and play a role in maintaining cell survival (Wang et al., 2020). Furthermore, CE-mediated recovery of CaM was impaired by 5-AZ, an inhibitor of Dnmts. These results suggest the importance of epigenetic modifications in regulating neuronal survival and provide clues to elucidate the mechanism underlying CE-induced neuroprotective functions. Due to the lack of information on the direct targets of CE on cells, further studies are needed to clarify the above issues. Furthermore, we noted that CE-induced restorative expression of PKC $\alpha$  and Bcl-2 was retained despite the inhibition of Dnmts (Figure 5), as PKC $\alpha$  and Bcl-2 can be activated by FGF2, as previously described, and can be continuously activated after CE incubation (Figure 3). Furthermore, it is noteworthy that Dnmt1 did not show reactive expression after CE incubation. Therefore, deciphering the unique features of Dnmts in neurons, especially their unique function in response to neurotoxic injury, is an interesting topic. A plausible explanation may be that neurons do not undergo mitosis and that Dnmt1 is responsible for maintaining methylation after DNA replication. However, a deeper understanding of Dnmts in neurons is needed, which may help to elucidate the epigenetic mechanisms of folk medicine on the nervous system.

## 5. Conclusion

In this study, we demonstrate that the FGF2-PI3K/Akt axis is one of the important signaling pathways for CE-mediated neuroprotection against STS-induced toxicity and apoptosis. CE has a strong signaling effect on the sustained expression of FGF2. In response to FGF2 stimulation, PI3K/Akt, Erk1/2 and PKC/CaM pathways were turned on to promote neuronal survival. Meanwhile, CE-mediated restoration of Dnmt3 suggests profound alteration to the genome through epigenetic modifications. Thus, this study illustrates the neuroprotective effect of CE against STS-mediated toxicity and its mechanism, paving a new avenue for pharmacological studies and therapeutic applications of the diseases in traditional medicine.

## Declarations

### Author contribution statement

Zhe-Ping Cai, Yun Yu, Rui-Yuan Pan: Performed the experiments; Analyzed and interpreted the data.

Chang Cao, Zhe Guo, Si-Jia Zhong: Performed the experiments.

Haowen Liang: Analyzed and interpreted the data; Wrote the paper.

Rongfeng Lan: Performed the experiments; Wrote the paper.

Xiao-Yan Qin: Conceived and designed the experiments; Analyzed and interpreted the data.

### Funding statement

This work was supported by the National Natural Science Foundation of China of China (Grant No. 81873088 and 21778038), and Shenzhen science and technology innovation committee program (JCYJ20180305163349116).

### Data availability statement

Data will be made available on request.

### Declaration of interests statement

The authors declare no conflict of interest.

### Additional information

Supplementary content related to this article has been published online at <https://doi.org/10.1016/j.heliyon.2021.e07503>.

## References

- Cannella, N., Oliveira, A.M.M., Hemstedt, T., Lissek, T., Buechler, E., Bading, H., Spanagel, R., 2018. Dnmt3a2 in the nucleus accumbens shell is required for reinstatement of cocaine seeking. *J. Neurosci.* 38, 7516–7528.
- Cheng, Y., Li, Z., Kardami, E., Loh, Y.P., 2016. Neuroprotective effects of LMW and HMW FGF2 against amyloid beta toxicity in primary cultured hippocampal neurons. *Neurosci. Lett.* 632, 109–113.
- Dehmelt, L., Halpain, S., 2005. The MAP2/Tau family of microtubule-associated proteins. *Genome Biol.* 6, 204.
- Ford-Perriss, M., Abud, H., Murphy, M., 2001. Fibroblast growth factors in the developing central nervous system. *Clin. Exp. Pharmacol. Physiol.* 28, 493–503.
- Guo, Z., Pan, R.Y., Qin, X.Y., 2013. Potential protection of *Coelogyssum viride* var. *bracteatum* extract against oxidative stress in rat cortical neurons. *J. Anal. Methods Chem.* 2013, 326570.
- Hemmings, B.A., Restuccia, D.F., 2012. PI3K-PKB/Akt pathway. *Cold Spring Harb Perspect. Biol.* 4, a011189.
- Herman, J.G., Graff, J.R., Myohanen, S., Nelkin, B.D., Baylin, S.B., 1996. Methylation-specific PCR: a novel PCR assay for methylation status of CpG islands. *Proc. Natl. Acad. Sci. USA* 93, 9821–9826.
- Hers, I., Vincent, E.E., Tavares, J.M., 2011. Akt signalling in health and disease. *Cell. Signal.* 23, 1515–1527.
- Hu, X.Q., Su, S.B., 2017. An overview of epigenetics in Chinese medicine researches. *Chin. J. Integr. Med.* 23, 714–720.
- Huang, S.Y., Li, G.Q., Shi, J.G., Mo, S.Y., 2004. Chemical constituents of the rhizomes of *Coelogyssum viride* var. *bracteatum*. *J. Asian. Nat. Prod. Res.* 6, 49–61.
- Jiemjit, A., Fandy, T.E., Carraway, H., Bailey, K.A., Baylin, S., Herman, J.G., Gore, S.D., 2008. p21(WAF1/CIP1) induction by 5-azacytosine nucleosides requires DNA damage. *Oncogene* 27, 3615–3623.
- Johnson-Farley, N.N., Patel, K., Kim, D., Cowen, D.S., 2007. Interaction of FGF-2 with IGF-1 and BDNF in stimulating Akt, ERK, and neuronal survival in hippocampal cultures. *Brain Res.* 1154, 40–49.
- Kostas, M., Lampart, A., Bober, J., Wiedlocha, A., Tomala, J., Krowarsch, D., Otlewski, J., Zakrzewska, M., 2018. Translocation of exogenous FGF1 and FGF2 protects the cell against apoptosis independently of receptor activation. *J. Mol. Biol.* 430, 4087–4101.
- LaPlant, Q., Vialou, V., Covington 3rd, H.E., Dumitriu, D., Feng, J., Warren, B.L., Maze, I., Dietz, D.M., Watts, E.L., Iniguez, S.D., et al., 2010. Dnmt3a regulates emotional behavior and spine plasticity in the nucleus accumbens. *Nat. Neurosci.* 13, 1137–1143.
- Li, M., Guo, S.X., Wang, C.L., Xiao, P.G., 2009. Quantitative determination of five glucosyloxybenzyl 2-isobutylmalates in the tubers of *Gymnadenia conopsea* and *Coelogyssum viride* var. *bracteatum* by HPLC. *J. Chromatogr. Sci.* 47, 709–713.

- Ma, B., Li, M., Nong, H., Shi, J., Liu, G., Zhang, J., 2008. Protective effects of extract of *Coeloglossum viride* var. *bracteatum* on ischemia-induced neuronal death and cognitive impairment in rats. *Behav. Pharmacol.* 19, 325–333.
- Okano, M., Bell, D.W., Haber, D.A., Li, E., 1999. DNA methyltransferases Dnmt3a and Dnmt3b are essential for de novo methylation and mammalian development. *Cell* 99, 247–257.
- Omura, S., Iwai, Y., Hirano, A., Nakagawa, A., Awaya, J., Tsuchiya, H., Takahashi, Y., Masuma, R., 1977. A new alkaloid AM-2282 of *Streptomyces* origin. taxonomy, fermentation, isolation and preliminary characterization. *J. Antibiot. (Tokyo)* 30, 275–282.
- Pan, R.Y., Ma, J., Wu, H.T., Liu, Q.S., Qin, X.Y., Cheng, Y., 2017. Neuroprotective effects of a *Coeloglossum viride* var. *bracteatum* extract in vitro and in vivo. *Sci. Rep.* 7, 9209.
- Qin, X.Y., Cui, J., Zhang, Y., 2010. *Coeloglossum viride* var. *bracteatum* extract protects against amyloid toxicity in rat prefrontal cortex neurons. *Int. J. Clin. Exp. Med.* 3, 88–94.
- Qin, X.Y., Lv, J.H., Cui, J., Fang, X., Zhang, Y., 2012. Curcumin protects against staurosporine toxicity in rat neurons. *Neurosci. Bull.* 28, 606–610.
- Rhee, I., Jair, K.W., Yen, R.W., Lengauer, C., Herman, J.G., Kinzler, K.W., Vogelstein, B., Baylin, S.B., Schuebel, K.E., 2000. CpG methylation is maintained in human cancer cells lacking DNMT1. *Nature* 404, 1003–1007.
- Schubert, D., Currais, A., Goldberg, J., Finley, K., Petrascheck, M., Maher, P., 2018. Geroneuroprotectors: effective geroprotectors for the brain. *Trends Pharmacol. Sci.* 39, 1004–1007.
- Shang, X., Guo, X., Liu, Y., Pan, H., Miao, X., Zhang, J., 2017. *Gymnadenia conopsea* (L.) R. Br.: a systemic review of the ethnobotany, phytochemistry, and pharmacology of an important Asian folk medicine. *Front. Pharmacol.* 8, 24.
- Tomomi, K., Ingraham, K.L., Jacobsen, M.T., Huangui, X., Tsuneya, I., 2011. FGF2 gene transfer restores hippocampal functions in mouse models of Alzheimer's disease and has therapeutic implications for neurocognitive disorders. *Proc. Natl. Acad. Sci. USA* 108, 19469–19470.
- Wang, M., Wu, X., Gan, L., Teng, Z., Zhang, H., Zhang, Y., 2020. Overexpression of Dnmt3a ameliorates diabetic muscle atrophy by modulating Pten/Akt pathway. *Exp. Physiol.*
- Yang, J., Tian, X., Yang, J., Cui, J., Jiang, S., Shi, R., Liu, Y., Liu, X., Xu, W., Xie, W., et al., 2017. 5-Aza-2'-deoxycytidine, a DNA methylation inhibitor, induces cytotoxicity, cell cycle dynamics and alters expression of DNA methyltransferase 1 and 3A in mouse hippocampus-derived neuronal HT22 cells. *J. Toxicol. Environ. Health A* 80, 1222–1229.
- Yang, X.P., Liu, T.Y., Qin, X.Y., Yu, L.C., 2014. Potential protection of 2,3,5,4'-tetrahydroxystilbene-2-O-beta-D-glucoside against staurosporine-induced toxicity on cultured rat hippocampus neurons. *Neurosci. Lett.* 576, 79–83.
- Zhang, D., Liu, G., Shi, J., Zhang, J., 2006a. *Coeloglossum viride* var. *bracteatum* extract attenuates D-galactose and NaNO<sub>2</sub> induced memory impairment in mice. *J. Ethnopharmacol.* 104, 250–256.
- Zhang, D., Liu, G.T., Shi, J.G., Zhang, J.J., 2006b. Effects of *Coeloglossum viride* var. *bracteatum* extract on memory deficits and pathological changes in senescent mice. *Basic Clin. Pharmacol. Toxicol.* 98, 55–60.
- Zhang, D., Zhang, Y., Liu, G., Zhang, J., 2006c. Dactylorhin B reduces toxic effects of beta-amyloid fragment (25-35) on neuron cells and isolated rat brain mitochondria. *N-S. Arch. Pharmacol.* 374, 117.
- Zhang, M., Yuan, T., 1998. Molecular mechanisms of calmodulin's functional versatility. *Biochem. Cell Biol.* 76, 313–323.
- Zhao, C., Yin, P., Mei, C., Li, N., Yao, W., Li, X., Qi, J., Fan, K., Li, Z., Wang, L., et al., 2013. Down-regulation of DNA methyltransferase 3B in staurosporine-induced apoptosis and its mechanism in human hepatocarcinoma cell lines. *Mol. Cell Biochem.* 376, 111–119.
- Zhong, S.J., Wang, L., Wu, H.T., Lan, R., Qin, X.Y., 2019. *Coeloglossum viride* var. *bracteatum* extract improves learning and memory of chemically-induced aging mice through upregulating neurotrophins BDNF and FGF2 and sequestering neuroinflammation. *J. Funct. Foods* 57, 40–47.